Small Damage Detection of Real Steel Bridge by using Local Excitation Method

Toshiyuki OSHIMA*, Yasunori MIYAMORI*, Shuichi MIKAMI*,
Tomoyuki YAMAZAKI* , Sherif BESKYROUN**, Maria FABIJANSKA KOPACZ***

* Department of Civil Engineering, Kitami Institute of Technology,
(165 Koencho, Kitami, Hokkaido, 090-8507, Japan)
oshima@mail.kitami-it.ac.jp
**The University of Auckland (20 Symonds Street, Auckland 1142, New Zealand)
s.beskyroun@auckland.ac.jp
***Cracow University of Technology (Warszaska 24 St., 31-155 Krakow, Poland)
fabijanska.maria@gmail.com

Abstract. By using piezoelectric actuator real steel bridge can be accelerated locally to detect the effect of small damage like fatigue crack and connection damage as a response change of vibration. Power spectrum density (PSD) function of the response can give us the indication of existence of damage before and after the damage. Detail analysis of PSD before and after damage can give us the location and size (area) of damage. Paper shows the experimental result of damage detection by using local excitation method on real bridge.

Keywords : Structural health monitoring , Local excitation, Power spectrum density(PSD)
Piezoelectric actuator, Vibration-based damage identification

1 Introduction

In recent years there has been interested in the damage diagnosis and health monitoring of existing bridges using vibration based damage identification techniques. Most vibration-based damage detection theories and practices are formulated based on the assumption that failure or deterioration would primarily affect the stiffness and therefore, affect the modal characteristics of the dynamic response of the structure[1-5]. If this kind of changes can be detected and classified, this measure can be further implemented for a bridge monitoring system to indicate the condition, or damage, or remaining capacity of the structure. However, conventionally defined modal parameters have been shown to be mildly sensitive in the detection of various types of bridge damages. Furthermore, the modal parameters of conventional modal testing such as frequencies and modal damping are global parameters, which cannot locate the damages[6]. Research efforts have been made to detect structural damage directly from dynamic response measurements in the time domain, e.g. the random decrement technique[7], or from frequency response functions (FRF)[8]. Also, some damage detection methods have been proposed to detect damage using system identification techniques[9, 10]. In this paper, an algorithm based on changes in Power Spectrum Density(PSD) is presented. The algorithm is used to detect damage, locate its position and monitor the increase in damage using only the measured data without the need for any modal identification or numerical models. The method is applied to the experimental data extracted from a railway steel bridge after inducing some defects to its members. A future goal of a comprehensive bridge management system is to have a self-monitoring bridge where sensors feed measured responses (accelerations, strains, etc.) into a local computer. This computer would, in turn, apply a damage identification algorithm to this data to determine if the bridge has significantly deteriorated to the point where user safety maybe jeopardized. One difficulty with determining dynamic parameters of a structure through ambient vibrations is that the forcing function is not precisely characterized. In this paper, the implementation of piezoelectric actuators[11-13] as a local excitation source for large structures such as steel bridges is presented. The advantages of using piezoelectric actuators instead of shakers, hammers or ambient vibrations will be discussed in details in the following chapters[14-21].

2 Damage Identification Algorithm

Many techniques have been proposed in the area of non-destructive damage detection using changes in modal parameters. However, in many structures only few modes are available which may decrease the accuracy of detecting and localizing damage using these techniques. In order to overcome the problem of the limited number of identified modal parameters, PSD information estimated from the various accelerometer readings at all frequencies in the measurement range and not just the modal frequencies will be compared before and after damage using the proposed method. PSD data can then be analyzed using statistical procedures to determine the damage location, as will be explained in details in this section.

PSD is determined from the acceleration time histories without the need to measure the excitation forces. Let $G_i(f)$ denotes the PSD magnitude measured at channel number i at frequency value f. The absolute difference in PSD magnitude before and after damage can then be defined as

$$D_i = \frac{\left| G_i(f) - G^*{}_i(f) \right|}{1 + \left| G_i(f) \right|} \qquad (1)$$

where $G_i(f)$ and $G_i^*(f)$ represent PSD magnitude for the undamaged and damaged structures, respectively. In the denominator of Eq.(1) 1 is added for analytical reason not to set zero just in case. The excitation forces used for the undamaged and damaged structure

must have the same amplitude, location and waveform in order to ensure that the changes in PSD data are mainly due to damage and not due to the change in excitation force characteristics. When the change in PSD is measured at different frequencies on the measurement range from f_1 to f_m , a matrix [**D**] can be formulated as follows

$$\mathbf{D} = \begin{bmatrix} D_1(f_1) & D_2(f_1) & ..... & D_n(f_1) \\ D_1(f_2) & D_2(f_2) & ..... & D_n(f_2) \\ . & . & ..... & . \\ . & . & ..... & . \\ . & . & ..... & . \\ D_1(f_m) & D_2(f_m) & ..... & D_n(f_m) \end{bmatrix} \qquad (2)$$

where n represents the number of measuring points. In matrix [**D**], every row represents the changes in PSD at different measuring channels but at the same frequency value. The summation of PSD changes over different frequencies can be used as the indicator of damage occurrence and the increase in damage. In other words, the first damage indicator is calculated from the sum of columns of matrix [**D**] as total change (**TC**)

$$\mathbf{SM} = \left\{ \sum_f D_1(f) \quad \sum_f D_2(f) \quad . \quad . \quad . \quad \sum_f D_n(f) \right\} \qquad (3)$$

Then total changes **SM** in PSD is calculated from the sum of columns of matrix [D] on each nodes.

However, it was found that total change **SM** is a weak indicator of damage localization. A statistical decision making procedure is employed to determine the location of damage. The first step in this procedure is the selection of the maximum change in PSD at each frequency value (the maximum value in each row of matrix [**D**]) and dividing all other changes in PSD measured at other nodes. For example in matrix [**D**], if $D_3(f_1)$ is the maximum value in the first row, then this value will be used as denominator $D_3(f_1)$ and all other values in this row are divided as shown in Eq.(4). The same process is applied to the different rows in matrix [**D**] to formulate the matrix of maximum changes of PSD at different frequencies, [C]

$$\mathrm{C} = \begin{bmatrix} C_1(f_1) = \dfrac{D_1(f_1)}{D_3(f_1)} & C_2(f_1) = \dfrac{D_2(f_1)}{D_3(f_1)} & \cdots & C_n(f_1) = \dfrac{D_n(f_1)}{D_3(f_1)} \\ C_1(f_2) = \dfrac{D_1(f_2)}{D_2(f_2)} & C_2(f_2) = \dfrac{D_2(f_2)}{D_2(f_2)} & \cdots & C_n(f_2) = \dfrac{D_n(f_2)}{D_2(f_2)} \\ \vdots & \vdots & & \vdots \\ \vdots & \vdots & & \vdots \\ C_1(f_m) = \dfrac{D_1(f_m)}{D_5(f_m)} & C_2(f_m) = \dfrac{D_2(f_m)}{D_5(f_m)} & \cdots & C_n(f_m) = \dfrac{D_n(f_m)}{D_5(f_m)} \end{bmatrix} \qquad (4)$$

In order to monitor the frequency of damage detection at any node, a new matrix [**C**] is formulated. This procedure can normalize the big differences over frequency ranges at each measuring nodes. For example in the matrix [**C**], a value of 1 is used corresponding to the locations of $C_3(f_1)$, $C_2(f_2)$ and so on, as shown in Eq.(4)

$$\mathbf{SC} = \left\{ \sum_f C_1(f) \quad \sum_f C_2(f) \quad . \quad . \quad . \quad \sum_f C_n(f) \right\} \tag{5}$$

Then **SC** is also the indicator of damage occurrence and it is called damage detection (**DD**) in this paper. The first damage localization indicator **D I 0** is defined as the scalar product of {***SM***} and {***SC***} as shown in the following expression;

$$\mathbf{D\ I\ 0} = \{ SM(1) \times SC(1) \quad SM(2) \times SC(2) \ldots \quad SM(n) \times SC(n) \} \tag{6}$$

In order to reduce the effect of noise or measurement errors, a value of one and two times standard deviation of the elements in vector {**SM**} will be subtracted from the vector {**SM**}. Any resulting negative values will be removed. The same procedure will be applied to the vector {**SC**} . Then Eq. (6) is modified for second and third damage location indicators **D I 1** and **D I 2** as follows;

$$\boldsymbol{SMD1} = \left\{ \sum_f D_1(f) - \sigma \quad \sum_f D_2(f) - \sigma \quad . \quad . \quad . \quad \sum_f D_n(f) - \sigma \right\} \tag{7}$$

where $\sigma = \sqrt{\sum_{i=1}^{n} (SM(i) - \overline{SM})^2} \Big/ (n-1)$, $\overline{SM} = \sum_{i=1}^{n} SM(i) \Big/ n$,

$$\boldsymbol{SCD1} = \left\{ \sum_f C_1(f) - \lambda \quad \sum_f C_2(f) - \lambda \quad . \quad . \quad . \quad \sum_f C_n(f) - \lambda \right\} \tag{8}$$

where $\lambda = \sqrt{\sum_{i=1}^{n} (SC(i) - \overline{SC})^2} \Big/ (n-1)$, $\overline{SC} = \sum_{i=1}^{n} SC(i) \Big/ n$.

The second damage localization indicator **D I 1** is defined as the scalar product of {***SMD1***} and {***SCD1***} as follows;

$$\mathbf{D\ I\ 1} = \{ SMD1(1) \times SCD1(1) \quad SMD1(2) \times SCD1(2) \ldots \quad SMD1(n) \times SCD1(n) \} \tag{9}$$

And for third damage location indicator **D I 2**

$$\boldsymbol{SMD2} = \left\{ \sum_f D_1(f) - 2\sigma \quad \sum_f D_2(f) - 2\sigma \quad . \quad . \quad . \quad \sum_f D_n(f) - 2\sigma \right\} \tag{10}$$

$$\boldsymbol{SCD2} = \left\{ \sum_f C_1(f) - 2\lambda \quad \sum_f C_2(f) - 2\lambda \quad . \quad . \quad . \quad \sum_f C_n(f) - 2\lambda \right\} \tag{11}$$

Then damage localization indicator **D I 2** is defined as the scalar product of {***SMD2***} and {***SCD2***} as follows;

$$\mathbf{D\ I\ 2} = \{ SMD2(1) \times SCD2(1) \quad SMD2(2) \times SCD2(2) \ldots SMD2(n) \times SCD2(n) \} \tag{12}$$

Damage localization indicators **D I 0** , **D I 1** and **D I 2** will be used to determine the damage location and the total change **TC** in PSD (Eq. (3)) and damage detection **DD**(Eq. (5) will be used to detect the occurrence of damage and monitor the growth in damage.

3 Experimental Setup and Equipment Arrangement for Damage Identification of Real Steel Railway Bridge

3.1 Bridge Dimension

Photo 1 Railway Bridge photo used for measurement
(Assembled steel I beam, length 6.96m Railway bridge)

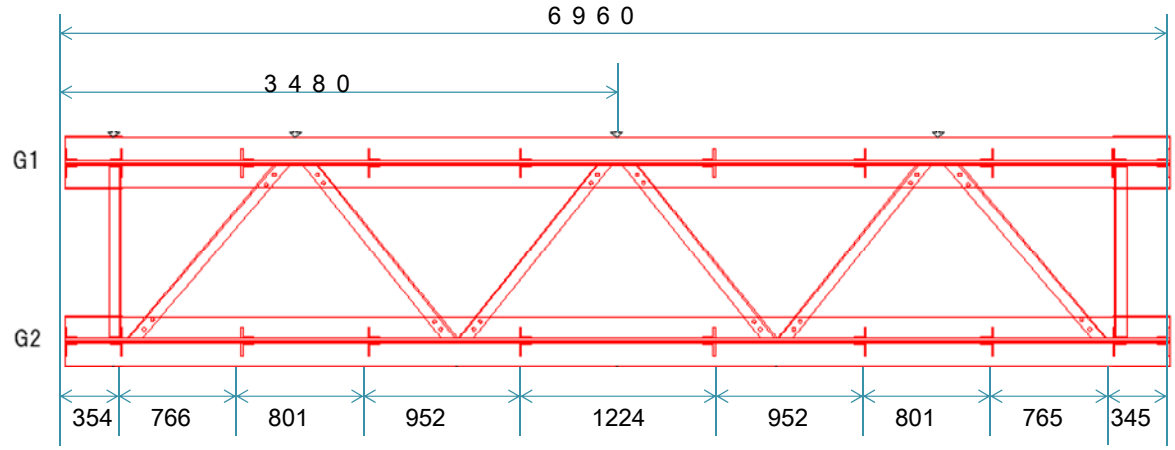

Fig. 1 Bridge dimensions (Unit: mm)

Table 1 Dimensions of assembled I beam girder

	Total length	6960
	Girder spacing	1127
Web	Length	6960
	Height	686
	Thickness	10
U-Flg	Length	6960
	Width	310
	Thickness	12
L-Flg	Length	6960
	Width	310
	Thickness	12
		(mm)

Bridge which was constructed in the year of 1909, has elements of 2 main girders (assembled I beams by rivets) and 2 diaphragms at the end of girder. Horizontal laterals are connected at the upper flange of girder by rivets as shown in Photo 1. In experiment bridge is supported on two wooden blocks at the end with fixation. Detail dimension of bridge is shown in Fig.1 and Table 1.
Cross sectional dimension(L type angle) of vertical stiffeners is 90× 80× 10(mm).

3.2 Sensor Arrangement

Sensors are 16 accelerometers and located in horizontal direction as shown in Fig. 2 and 3. Actuator is set on the center of web plate at the middle of G1 girder between ch7 and ch8 in horizontal direction as shown in Fig. 2 and Photo 2. Then out of plane vibration of web plate is generated by this setup.

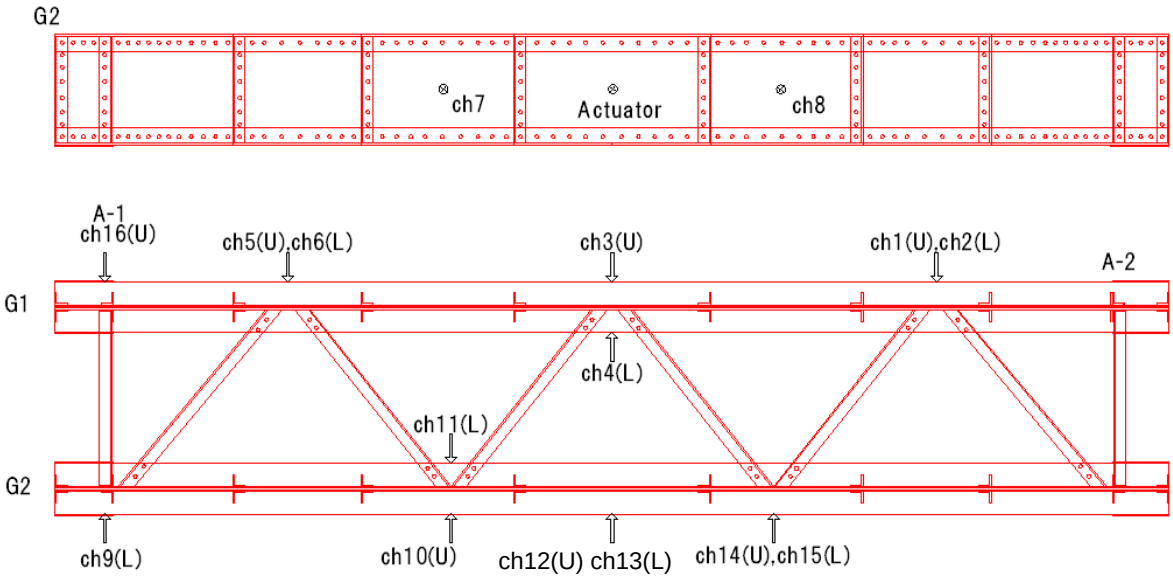

Fig. 2 Sensor locations on horizontal plane

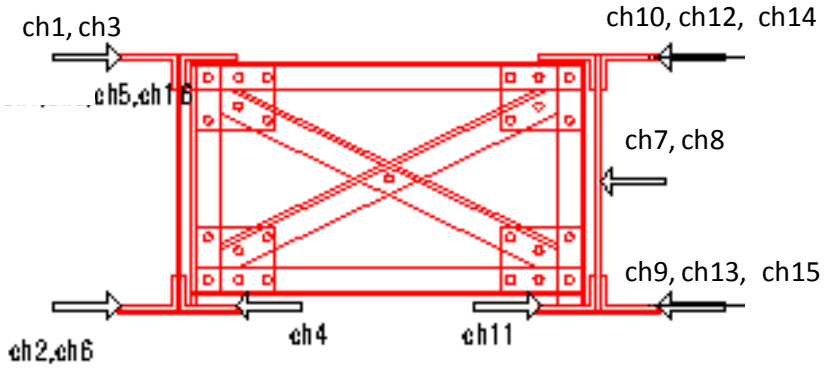

Fig. 3 Sensor locations on cross sectional plane

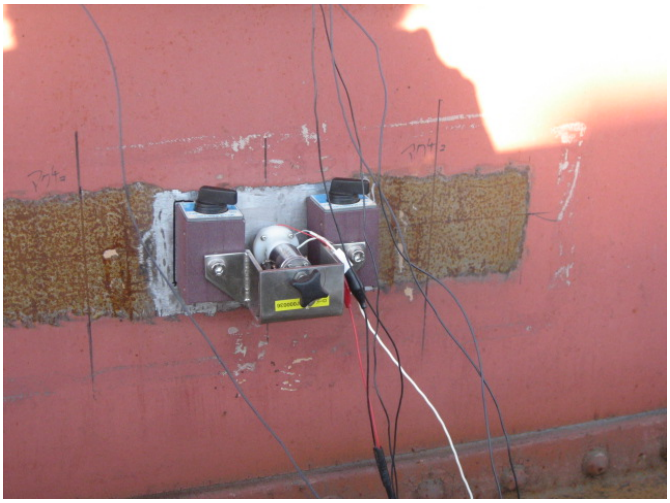

Photo 2 Actuator set on center of web plate in the middle of G1 girder

Excitation: Piezoelectric actuator is permanently fixed at the center point of the web plate of G1 girder. Excitation force amplitude is 30 (N). Excitation force direction: horizontal, Excitation wave form: sine sweep, Excitation frequency: 1~750Hz, Excitation time 20 sec, recording time: 25 sec, sampling rate: 10000 Hz.

[1] Piezoelectric actuator: A wave function generator is used to adjust the required excitation frequency range, the time in which the actuator reaches the maximum frequency and the excitation wave form. Then, the adjusted wave is transferred to the power supplier which in turn provides the actuator with the adjusted power. The actuator is fixed to the structure by a magnetic holder. This magnetic holder is suitable for fixing the actuator to steel structures; A steel spring is fixed over the actuator to control the excitation force amplitude. The produced force amplitude is constant but the excitation frequency gradually increases over time until it reaches its maximum value after the designated time. It should also be noted that because the actuator is pressed but not glued to the test structure, the actuator provides pressure force only. The excitation frequency is gradually increasing over time until it reaches its maximum value after the designated time (20 seconds in this case). In this case, the excitation wave form is a sweep function.
[2] Piezoelectric accelerometer: The accelerometer has a nominal sensitivity of 10 mv/g, a specified frequency range of 5~4000Hz and an amplitude range of 200 m/s^2.

4 Small Crack Detection of Real Bridge (Damage 1)

4.1 Damage Details for Crack

Artificial crack is made at the center of girder G1 of the outer lower flange plate as shown in Fig. 4. Location is the opposite side of accelerometer **ch4** and beneath **ch 3** in the lower flange plate of girder G1. Length of artificial damage crack is chosen as one fourth of the flange width for **Case 1** and one half of flange width for **Case 2** as shown in Photo 2. Crack is clearly opened without contact between their side surfaces. Environmental temperature around the bridge and meassument equipment is measured as 23 ℃ during the measurement.

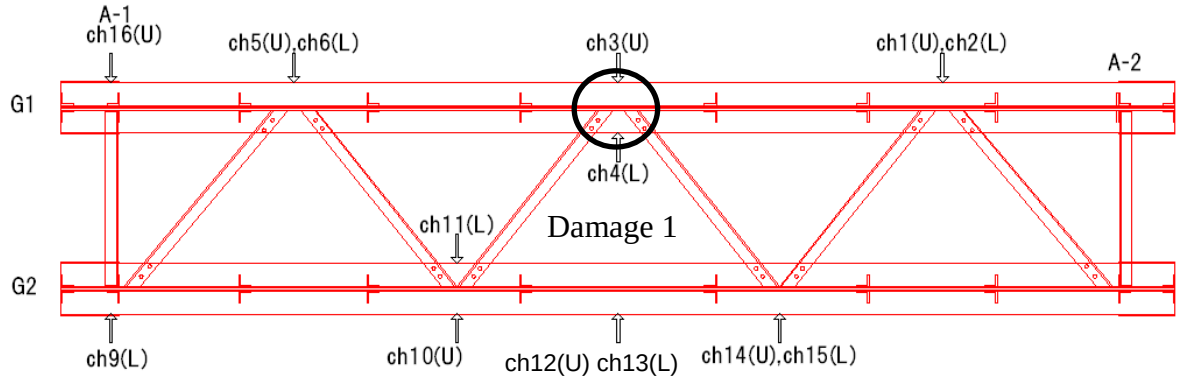

Fig. 4 Location of artificial damage crack on girder G1

Photo 3 Artificial Crack of **Case 1** by one fourth of flange width

Photo 4 Artificial Crack of **Case 2** by one half of flange width

4.2 Damage Identification in the case of Damage 1(Crack)

In the case of Damage 1 (crack case) Eq. (3) is slightly changed as shown in Eq. (13). Local excitation by actuator is set on the girder G2 which is opposite location from girder G1 where the crack damage is located. The reason why the artificial crack is made on the opposite side girder G1 is that how the detection by this damage identification algorithm works even in the case when distance between excitation and damage are not close. The effect of small crack in

the vibration data is small and analysis is focused on how analytical method can detect the small damage of crack. In order to distinguish the effect of small crack in the analysis, the denominator of Eq. (3) is chosen as a smaller value from the PSD value over each frequency and channel of both before and after damage as shown in Eq. (13).

$$D = \frac{|G_i(f) - G^*{}_i(f)|}{1 + (G_i(f), G^*{}_i(f))_{\min}} \quad (13)$$

The total change (**TC**) calculated by Eq. (3) in **Case 1** of Damage 1 is shown in Fig. 5 and the damage detection (**DD**) given by Eq. (5) is shown in Fig. 6

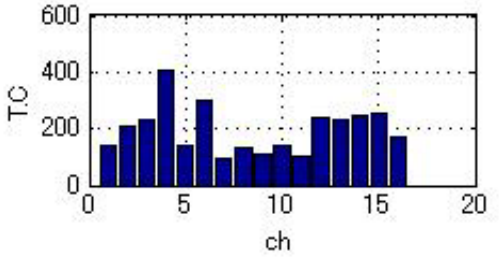

Fig. 5 Total change (**TC**) in **Case 1** of Damage 1

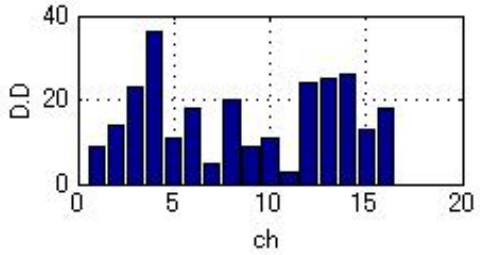

Fig. 6 Damage Detection (**DD**) in **Case 1** of Damage 1

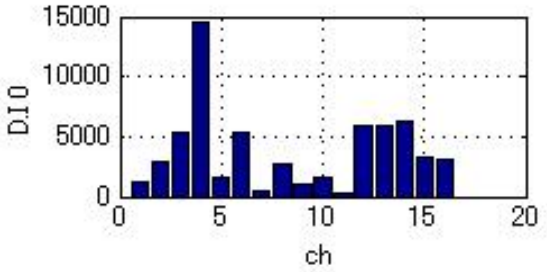

Fig. 7 Damage Indicator **D I 0** in **Case 1** of Damage 1

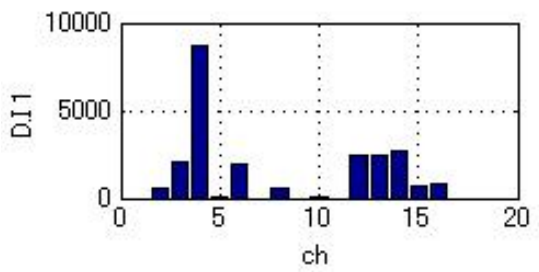

Fig. 8 Damage Indicator **D I 1** in **Case 1** of Damage 1

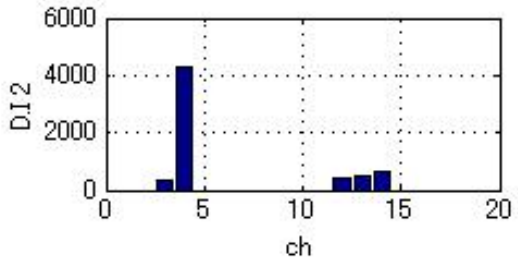

Fig. 9 Damage Indicator **D I 2** in **Case 1** of Damage 1

And the damage indicator **D I 0**, **D I 1** and **D I 2** given by Eq. (6) , Eq. (9) and Eq. (12) in **Case 1** are shown in Fig. 7, Fig. 8 and Fig. 9. In Fig. 9 by using **D I 2** the location of the crack is clearly identified .

For **Case 2** of Damage 1 the total change (**TC**) is shown in Fig. 10 and the damage detection (**DD**) is shown in Fig. 11.

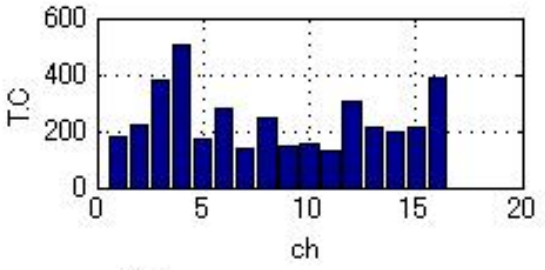

Fig. 10 Total change (**TC**) in **Case 2** of Damage 1

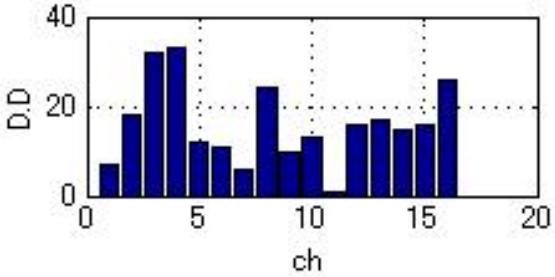

Fig. 11 Damage Detection (**DD**) in **Case 2** of Damage 1

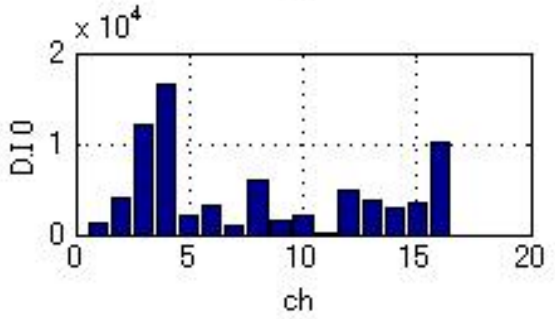

Fig. 12 Damage Indicator **D I 0** in **Case 2** of Damage 1

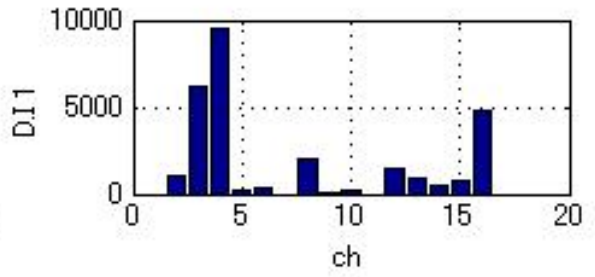

Fig. 13 Damage Indicator **D I 1** in **Case 2** of Damage 1

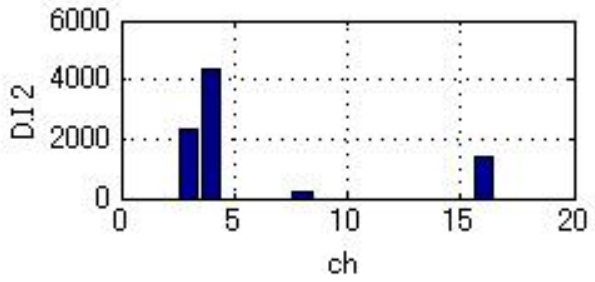

Fig. 14 Damage Indicator **D I 2** in **Case 2** of Damage 1

The damage indicator **D I 0**, **D I 1** and **D I 2** in **Case 2** of Damage 1 are shown in Fig. 12, Fig.13 and Fig. 14. In Fig.14 by using **D I 2** the location of the crack is also clearly identified as on channel 3 and channel 4 . By comparing the results on both cases of **Case1** and **Case2** of Damage 1 the influence of bottom crack in vibration data is more distributed over to the other portion of girders due to the size of crack.

5 Damage Detection of Connection on Lateral Member (Damage 2)

5.1 Damage Details for Connection

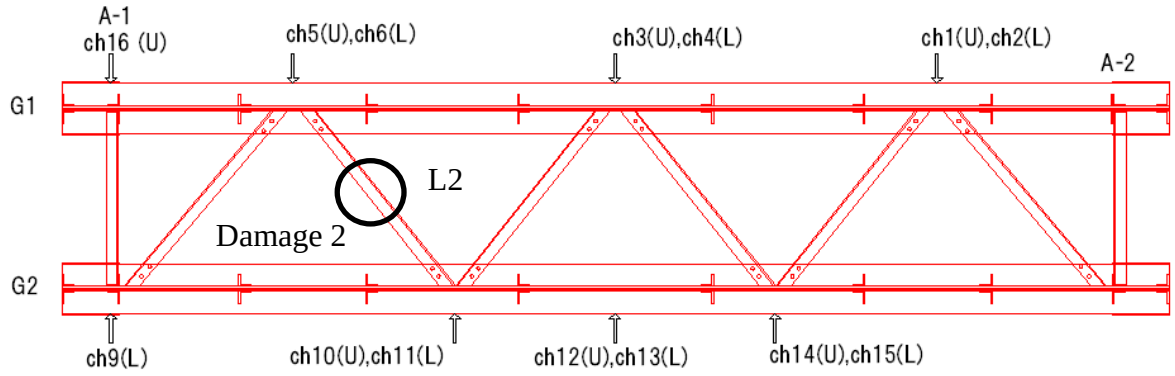

Fig. 15 Location of artificial damage of connection on lateral member L2

Artificial damage is chosen to cut at the center of the lateral member between ch5 and ch10 as shown in Fig.15 and Photo 3. And after cutting full splice connection was done as shown in Photo 4. This condition is chosen as a healthy condition without damage as **D0.**
And by removing splice bolts damage cases **D1** and **D2** are chosen as shown in Photo 5 and Photo 6.

Photo 3 Full cut of cross section of lateral member L2

Photo 4 Splice connection of lateral member by bolts (**D0**)

Photo 5 Damage **D1** by removing outside 2 bolts at vertical splice

Photo 6 Damage **D2** by removing all bolts at vertical splice

5.2 Damage Identification in the case of Damage 2 (Connection)

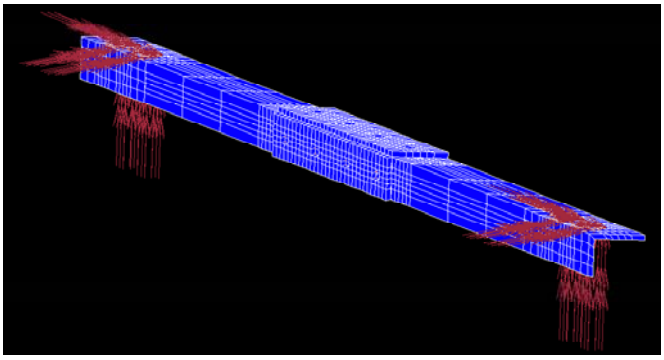

Fig.16 FEM modeling of lateral member with splice connection

Table 2 Modal frequency before and after damage

	D0	D1
1st	142.2	126.1
2nd	188.8	180.9
3rd	291.1	274.2
4th	491.8	430.2
5th	569.9	447.1
6th	940.5	629.5
		(Hz)

Measured frequency range by accelerometer is 0Hz to 750Hz. As shown in Eq. (2) and Eq. (4) damage effect should be detected in this range of frequency. In order to make sure this range of frequency FEM modeling of only lateral member and modal analysis was done as shown in Fig. 16 and Table 2. Connection force by bolt is modeled by spring force between plates around splice holes. Supporting condition on both ends of member is fixed.
Numerical results are shown in Table 2 in the cases of **D0** and **D1**. So that we can estimate that the target range of frequency to use in the analysis is in around 100Hz – 700Hz.

Analyzed results for **SM**(Total change) by Eq. (3) is obtained and then damage indicators **DI2** by Eq. (12) are shown in Fig. 17 and Fig. 18 in cases of damages **D1** and **D2**. Information of damage existence in case of smaller damage **D1** is given at channel 11 which locates on lower flange of main girder as shown in Fig. 5. On the other hand, in case of larger damage **D2** larger influence of damage locates more at channel 5, 7 10 and 11 as shown in Fig. 18. By array distribution measurement through local excitation of external force we can get clear information on damage even if damage is smaller. Decision of array distribution of sensors is important in the area of suspected damage region of structure.

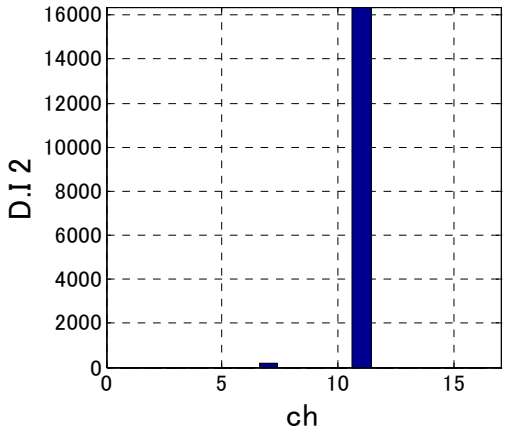

Fig. 17 DI2 for Case D1

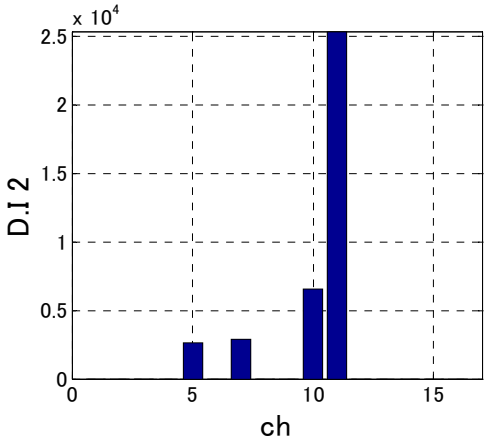

Fig.18 DI2 for Case D2

6 Final Remarks

It is shown that by array sensing through local excitation using piezoelectric actuator we can get the local damage information properly. It is important to detect the smaller damage as soon as possible when it is occured. In the structural health monitoring of bridge the initial structural condition is measured and after damage progressed the damaged condition is again measured to compare with initial condition. Just after new bridge construction the masurement on undamaged condition for the structure is desirable as the data of initial condition. But generally initial condition is measured when the damage is found and the damage progress is monitored by the succesive mesurement on damaged structure. Numerical analysis for undamaged and damaged condition of structure gives the accessment on the result of measurement.

To detect the smaller damage properly it is also important to measure the damaged condition under same temperature and same suructural boundary conditions as the initial condition was measured. In our experience of measurement the environmental temperature difference between initial condition and damaged condition should be less than 10 ℃ and 5 ℃ is recommended if it is possible.

Distribution of array sensors in the measurement is important and location of excitation effects also on the accuracy of the results. Normally damage is hidden behind the details of the structure, so that the location of excitaion should be moved in the area of suspected damages and their average of the result of damage indicator over the moved locations of excitation gives more acurate imformation of the damage.

This research also aims at establishment of experimental environment to enable the verification of applicability and the effective evaluation of the structural health monitoring (SHM) technology that uses the high performance sensor system on real bridges. The primary goal of the this project is the development of test beds that meet wider needs for SHM experiments. Several steel bridges on an abolished railway in Hokkaido, Japan are available in this test beds. The test beds can be utilized by not only researchers of this project but also other researchers. The final goal of the project is the international collaboration by means of cooperative utilization of the test beds. This research was supported by JST(Japan Science and Technology) Agency as international collaboration during 2007 to 2010. Authors acknowledged to their support on this project.

References

[1] Doebling S. W., C. R. Farrar, M. B. Prime, and D. W. Shevitz, 1996. *Damage Identification and Health Monitoring of Structural and Mechanical Systems from Changes in their Vibration Characteristics*, A Literature Review, Los Alamos National Laboratory Report, LA-13070- MS .

[2] Farrar C. R. et al., 1994. *Dynamic Characterization and Damage Detection in the I-40 Bridge Over the Rio Grande*, A Literature Review, Los Alamos National Laboratory Report, LA-12767- MS .

[3] Farrar C. R. and D. A. Jauregui, 1996. *Damage Detection Algorithms Applied to Experimental and Numerical Model Data from the I-40 Bridge*, Los Alamos National Laboratory Report, LA-12979-MS .

[4] Sampaio R. P. C., Maia N. M. M. and Silva J. M. M., 1999. Damage detection using the frequency-response-function curvature method, *Journal of Sound and Vibration*, 226(5), pp. 1029-1042 .

[5] Peeters B., Maeck J. and De Roeck G., 2001. Vibration-based damage detection in civil engineering: excitation sources and temperature effects, *Smart Materials and Structures*, 10, pp.518-527 .

[6] Xue S. T. , N. Fujitani, Z.B. Wei and H.S. Tang, 2006. Comparison of variations of natural frequencies for wooden structural models with and without damages part 2, shaking table based results, *Proceedings of the international conference on Structural Health Monitoring and Intelligent Infrastructure*, China, pp 1101-1104 .

[7] Yang J. C. S. , J. Chen and N. G. Dagalakis, 1984. Damage detection in offshore structures by the random decrement technique, *Journal of Energy Resources Technology*, American Society of Mechanical Engineers 106, 38-42 .

[8] Flesch R. G. and K. Kernichler, 1988. Bridge inspection by dynamic tests and calculations dynamic investigations of Lavent bridge, *workshop on Structural Safety Evaluation Based on System Identification Approaches* (H. G. Natke and J. T. P. Yao, editors), 433-459, Lambrecht/ Pfalz, Germany: Vieweg & Sons.

[9] Masri S. F. , R. K. Miller, A. F. Saud and T. K. Caughey, 1987. Identification of nonlinear vibrating structures, *Journal of Applied Mechanics 54*, 923-929: Part I-formulation .

[10] Natke H. G. and J. T. P. Yao, 1990. System identification methods for fault detection and diagnosis, *International Conference on Structural Safety and Reliability*, American Society of Civil Engineers, New York, 1387-1393 .

[11] Oshima T., Yamazaki T., Onishi K. and Mikami S., 2002. Study on damage evaluation of joint in steel member by using local vibration excitation, (In Japanese), *Journal of Applied Mechanics , JSCE*, Vol.5, pp.837-846 .

[12] Beskhyroun S., Oshima T., Mikami S., Yamazaki T., 2003. Damage detection and localization on structural connections using vibration based damage identification methods, *Journal of Applied Mechanics, JSCE*, Vol.6, pp. 1055-1064 .

[13] Beskhyroun S., Mikami S., Oshima T. and Yamazaki T., 2004. Modified damage identification algorithm based on vibration measurements, *Journal of Applied Mechanics, JSCE*, Vol.7, pp. 97-107 .

[14] Beskhyroun S., Oshima T., Mikami S., Tsubota Y., 2005. Structural damage identification algorithm base on change in power spectral density , *Journal of Applied Mechanics, JSCE*, Vol.8, pp. 73-84 .

[15] Beskhyroun S., Mikami S., Oshima T., 2006. Structural damage detection and localization using changes in phase angle, *Journal of Structural Engineering, JSCE*, Vol.52A, pp. 659-670 .

[16] Beskhyroun S., Mikami S., Oshima T. , 2006. Nondestructive damage detection scheme for steel bridges, *Journal of Applied Mechanics, JSCE*, Vol.9, pp. 63-74 .

[17] Mikami S., Beskhyroun S., Miyamori Y., Oshima T., 2007. Application of a vibration-based damage detection algorithm on a benchmark structure , Structural Health Monitoring of Intelligent Infrastructure, Vol.3 , CD ROM(No. 55) .

[18] Mikami S., Beskhyroun S., Yamazaki T., Oshima T., 2007. Damage detection in concrete structure using tunable piezoelectric actuators, *Journal of Applied Mechanics, JSCE*, Vol.10, pp.77-88 .

[19] Mikami S., Beskhyroun S., Oshima T. , 2011. Wavelet packet based damage detection in beam-like structure without baseline modal parameters, *Journal of Structure and Infrastructure Engineering, Maintenance, Management, Life-Cycle Design and Performance*, Vol.7, pp. 211-227 .

[20] Kumar R. P., Oshima T., Yamazaki T., Mikami S., Miyamori Y., 2012. Detection and localization of small damages in a real bridge by local excitation using piezoelectric actuators, *Journal of Civil Structural Health Monitoring*, Vol.2, No. 2, pp. 97-108 .

[21] Beskhyroun S., Oshima T., Mikami S., Miyamori Y., 2013. Assessment of vibration-based damage identification techniques using local excitation source , *Journal of Civil Structural Health Monitoring*, In printing .